Structure and stability of DPPE planar bilayers

Barry Stidder,[ab] Giovanna Fragneto*[a] and Stephen J. Roser[b]

Received 30th August 2006, Accepted 17th October 2006
First published as an Advance Article on the web 10th November 2006
DOI: 10.1039/b612538g

Biomembrane mimics in the form of supported planar bilayers allow the application of a wide range of surface and interface analytical techniques. The structure and phase-behavior of single and double bilayers of 1,2-dipalmitoylphosphoethanolamine (DPPE) were investigated by specular neutron reflectivity for their viability as biomembrane mimics. Whilst single bilayer samples were found to exhibit stable gel and fluid structures, double bilayers were found to be intrinsically unstable in the fluid phase as a planar structure. A Bragg peak was observed in the reflectivity data at just above the gel-to-fluid transition temperature, indicating the partial rearrangement of the upper bilayer into a repeat stacked structure. The lower bilayer was structurally stable. The structure and phase-behaviour of a double bilayer containing a ratio of 9 : 1 DPPE/cholesterol was also investigated to assess the stabilising effect of cholesterol on the upper bilayer. The presence of cholesterol completely destabilised the upper bilayer, causing it to detach 7 °C below the gel-to-fluid transition temperature of DPPE. It is possible that the cholesterol increases the overall conical shape of DPPE molecule by residing in the chain region of the lipid.

Introduction

To exploit certain types of surface and interfacial techniques in biological cell membrane studies it is necessary to use planar lipid bilayers located on or near to a substrate. These planar systems have allowed the application of AFM,[1] impedance analysis,[2,3] surface plasmon resonance,[4] neutron reflectivity,[5,6] and ellipsometry.[7] Examples of types of planar systems range from single bilayers adsorbed or deposited onto substrates[2,8–10] to multilamellar stacked bilayers[11,12] to elaborate polymer supported bilayers[13–15] and hybrid bilayers with one leaflet of lipids and the other of alkanethiols.[16]

One of the main advantages of single bilayer samples compared to multilamellar samples is that the information obtained is bilayer specific; it is not the average of hundreds or thousands of bilayers. Another advantage is that very low concentrations are needed to fabricate these samples. This is obviously interesting when expensive components are being studied. Often the main disadvantage of single bilayer systems is that the substrate can exert a restraining force upon the bilayer, inhibiting its phase behavior. Another key disadvantage is that only a very thin water layer separates the bilayer from the substrate (5–10 Å). This can restrict the inclusion of transmembrane proteins that protrude either side of the bilayer.[14]

To overcome some of the problems associated with single bilayer systems, a new type of planar membrane system has been developed. It consists of a bilayer floating above another bilayer that is in close proximity to the substrate.[5] Fabrication is achieved by a combination of Langmuir–Blodgett and Langmuir–Schaefer depositions. These techniques enable the fabrication of asymmetric bilayers where the composition of each leaflet can be selected to model the asymmetric nature of real membranes. Compared to single bilayer samples the upper bilayer is less constrained and is open to a large reservoir of water, making it ideally suited to study transmembrane phenomena and translocation. When the double bilayers are fabricated with phosphatidylcholines, the upper bilayer is separated from the lower bilayer by a water layer of 20–30 Å, whilst the lower bilayer is separated from the substrate by a water layer of 5–10 Å.[17] The upper bilayer exhibits comparable gel, transition and fluid phase-behaviour to vesicles in solution.[18] During phase-behavior studies, the main water layer was found to swell around the main transition temperature. This was interpreted in terms of competition between the inter-bilayer potential and membrane fluctuations and used to estimate the bending rigidity of the bilayer.[17] Off-specular synchrotron radiation measurements have allowed the measurement of the bending modulus and tension of the floating bilayer.[19] Incorporation of low concentrations of cholesterol (1–6 mol%) was found to progressively decrease the swelling,[20] and at a concentration of 10 mol% swelling was completely removed.[21]

Together with phosphatidylcholines, phosphatidylethanolamines are one of the most abundant components of the lipid bilayer in membranes and can even be found to account for up to a third of the total percentage of lipids present, as in the case of human and the rat erythrocyte plasma membranes. They are often found asymmetrically distributed in membranes, being predominantly located in the inner cytoplasm-facing leaflet. As well as being one of the major building blocks of membranes, they also have specific tasks such as supporting active transport by the lactose permease. They also act as a chaperone during the assembly of membrane proteins, guiding the folding path and aiding in the transition from the

[a]*Institut Laue-Langevin, 6 rue Jules Horowitz, b.p. 156, 38042, Grenoble, France. E-mail: Fragneto@ill.fr; Fax: +33 476207120; Tel: +33 476207062*
[b]*Department of Chemistry, University of Bath, Bath, UK, BA2 7AY. E-mail: s.j.roser@bath.ac.uk; Fax: +44 1225386231; Tel: +44 1225386569*

cytoplasmic to the membrane environment. In comparison to phosphatidylcholines, the smaller head-group of phosphatidylethanolamines enables stronger hydrogen bonds between the phosphate oxygen and the primary amine parts of the lipids.[22] Despite their predominance, phosphatidylethanolamines have not received as much attention as phosphatidylcholines in the literature. The phase-behaviour of phosphatidylethanolamines vesicles has been well characterised, whilst literature on the behaviour of stacked multilamellar bilayers is rather limited. With a view to the application of phosphatidylethanolamine double bilayers as planar biomembrane mimics, the phase-behaviour of DPPE single and double bilayers was investigated by neutron reflectivity. Double bilayers with a ratio of 9 : 1 DPPE/cholesterol were also studied with the dual purpose of assessing the stabilising effect of cholesterol on the upper bilayer and to increase the realism of the mimic by increased number of components. We have already shown that asymmetric double bilayers containing DPPE can be prepared and are stable in both the gel and fluid phases.[20]

Like their phosphatidylcholine counterparts, phosphatidylethanolamine vesicles are known to exhibit stable lamellar gel and liquid phases. However, they do not exhibit transition phase-behaviour like the ripple structure.[23] In the gel phase the lipids are highly ordered with restricted mobility, whilst in the fluid phase they are disordered and have greater freedom of movement. The bilayer in the fluid phase is thinner than in the gel phase. The temperature at which the gel-to-fluid transition occurs in phosphatidylethanolamine bilayers is usually higher than that for similar phosphatidylcholine bilayers, due to the stronger hydrogen bonding between the lipids. Certain types of phosphatidylethanolamines exhibit a transition from lamellar liquid phases to a non-lamellar inverted hexagonal phase at high temperatures.[24,25] Non-lamellar phases such as these have been found in vital cell tasks, such as in cell division where a non-lamellar phase forms around the area in the membrane where the cell is splitting with another cell. A similar effect also occurs in cell fusion.[26] Inverted hexagonal phases consist of hexagonally arranged rods of lipids with water channels inside.[27] The water core is circular up to a certain radius limit, above which it is deformed due to packing difficulties.[28] The fluid-to-inverted hexagonal transition (T_h) normally happens at significantly higher temperatures than the gel-to-liquid transition (T_m). For example, DSPE (C_{18}) has a T_m of 75.5 °C and a fluid-to-inverted hexagonal temperature of 109.5 °C.[29] DPPE has a well defined T_m of 64.5 °C and T_h of 123 °C.[24] Contrary to the trend that an increase in chain length increases the value of T_m, T_h actually decreases with increasing chain length.

Cholesterol is known to have a stabilising effect on cell membranes, increasing their fluidity at low temperature and restricting it at higher temperatures.[30] Studies of phosphatidylethanolamines and cholesterol mixtures are rather limited in the literature, despite the abundance of phosphatidylethanolamines in membranes.[31] Previous studies have shown cholesterol to have a greater effect on transition temperatures of phosphatidylethanolamines compared to phosphatidylcholines. Addition of cholesterol to DPPE vesicles leads to a continuous decrease and broadening of T_m, whilst by a concentration of 50 mol% no detectable T_m is observed. The transition enthalpy also decreases almost linearly with increasing concentration.[22] Inclusion of 30 mol% cholesterol into DOPE vesicles was found to lower the lamellar-to-hexagonal transition (T_h) by ~30 °C.[32] The reduction in T_m and T_h with increasing cholesterol concentration is thought to be due to the cholesterol molecules interfering with the hydrogen bonding of the phosphatidylethanolamines head-groups. However, it is not possible to generalise the effect of cholesterol on the behaviour of phospholipids as it varies appreciatively with the head-group structure and the chain structure and length.[33]

Supported single bilayers and monolayers of phosphatidylethanolamines have been used in a limited number of studies; examples include the interaction of key proteins involved in cell division with supported bilayers of DPPE[34] and studies of the interactions of antimicrobial peptides with DPPE monolayers.[35] AFM studies have been used to map the adhesive forces between deposited DMPE monolayers and surfaces.[36]

Experimental

Lipids and substrates

DPPE (purity ⩾ 99%) and cholesterol (purity ⩾ 99%) were purchased from Sigma Chemicals. All chemicals were used without further purification. The silicon substrates (8 × 5 × 2 cm^3) were polished on one side to an average root-mean-square roughness of 3 Å by the ESRF optics laboratory (Grenoble, France). Prior to deposition, the silicon substrates were cleaned separately in chloroform, ethanol, and ultra-pure water in an ultrasound bath for 15 minutes per solvent. All solvents used were of analytical grade. Ultra-pure water was of Millipore grade (18 MΩ cm) and the D_2O of 99% purity was supplied by the Institut Laue-Langevin, Grenoble. A highly hydrophilic surface was formed on the silicon substrates by exposure to UV/ozone for 30 minutes.[37] The substrates were deposited on this surface immediately after.

Bilayer deposition

Fabrication of the double bilayers involves three vertical Langmuir–Blodgett (LB) monolayer depositions and one horizontal Langmuir–Schaefer (LS) deposition.[5] Single bilayers are fabricated *via* a vertical LB deposition followed by a horizontal LS deposition. Monolayers of the components are first formed by dissolving the components in chloroform and spreading on a Langmuir trough (Nima technology, Coventry, UK), allowing 20 minutes for the solvent to evaporate. To dissolve DPPE in chloroform, mild heating (~35 °C) is necessary. LB depositions were performed at 17 °C using a deposition speed of 5 mm min^{-1} and constant surface pressure of 40 mN m^{-1}. The LS deposition needs excellent horizontality of the sample and a very low contact speed of 20 microns per second. To achieve this, an in-house-built micro-table-controlled manual dipper with precision-adjusted verticality was developed. Once fabricated, the samples were sealed under water in 10 mL reservoirs ready for reflectivity measurements.

Prior to reflectivity measurements, Langmuir–Blodgett monolayer depositions of 0 mol%, 5 mol%, 10 mol% and

30 mol% cholesterol/DPPE were evaluated to assess their fabrication. All gave successful depositions, characterised by a high transfer ratio for the second and third layers.

Neutron reflectivity measurements

Specular neutron reflectivity is a non-destructive technique widely used in soft matter studies for determining the structure of layers at a surface or a buried interface.[38,39] Structural information such as the composition, internal dimensions and interfacial roughness are obtained. Measurements can be performed *in situ* and only very small amounts of material are required, which is highly advantageous when using expensive components. Neutron scattering techniques are particularly suitable to biological systems as, unlike in X-ray scattering, elements such as hydrogen, carbon, oxygen, and nitrogen are strong scatterers and different isotopes of the same element have different scattering lengths. This enables the use of contrast variation and isotopic labelling of parts of the interface, where components can be exchanged for their isotopic counterpart, giving a similar structure but with a different scattering length density, thus allowing high resolution determinations.[31] Specular neutron reflectivity $R(Q)$, defined as the ratio between the reflected and incoming intensities of a neutron beam, is measured as a function of the wave-vector transfer $Q = 4\pi/\lambda\sin\theta$ (where λ is the wavelength and θ the angle of the incoming beam to the surface) perpendicular to the interface. In the kinematic or Born approximation,[40] for an ideal interface, the reflectivity is related to the scattering length density (SLD) by

$$R(Q) \approx \frac{16\pi^2}{q^4}\mathrm{SLD}^2$$

and the scattering length density is related to the composition density by

$$\mathrm{SLD} = \sum_{\mathrm{j}} b_{\mathrm{j}} n_{\mathrm{j}}$$

where b_j is the scattering length of nucleus j and n_j is the number of nuclei per unit volume. Neutron specular reflectivity measurements were performed on the high flux D17 reflectometer[41] at the Institut Laue-Langevin (Grenoble, France) in time-of-flight mode using a spread of wavelengths between 2 Å and 20 Å with two incoming angles of 0.7° and 4°. The reflectivity was measured upon heating and cooling between 25 °C to 84 °C to 25 °C. This range covered the main gel, transition and fluid phase temperatures. All samples were allowed to equilibrate for 15 minutes at each temperature before the reflectivity profile was measured.

Reflectivity data analysis

The method of analysis often used for specular reflection data involves the construction of a model of the sample, which is then parsed into a series of parallel layers of homogeneous material. Each layer is characterised by an SLD and a thickness, which are used to calculate a model reflectivity profile by means of the optical matrix method.[40] The interfacial roughness between any two consecutive layers may also be included in the model by the Abeles method. The parameters of the model are varied within physically realistic constraints until the calculated reflectivity profile matches the measured profile. The double bilayer sample is separated into homogeneous layers as follows. Each bilayer is divided into a homogeneous chain-region layer and two head-group layers. The water layers separating the bilayers and the lower bilayer from the substrate constitute two more layers. The thin silicon oxide layer is treated as one layer. The scattering length densities used for each layer are listed in Table 1. They are assumed not to vary significantly within the temperature range studied and are therefore kept constant. When the double bilayer containing 10 mol% cholesterol is modelled, the cholesterol is assumed to be predominantly located in the hydrophobic chain region of the bilayer.[42] Therefore the scattering length density of this layer is adjusted to account for the effect of the concentration and volume of the cholesterol. The error margins of the fitted parameters are the error in the modelled parameters.

Results and discussion

Phase-behavior of DPPE single bilayers

The structure and stability of DPPE single planar bilayers were determined at gel and fluid phase temperatures ranging from 25 °C to 79 °C. Fitted profiles of the lowest and highest temperatures measured are given in Fig. 1. Structural parameters are listed in Table 2.

The bilayer thickness (Db) remained constant throughout the gel phase temperature range. The bilayer chain-region thickness was comparable to twice the calculated maximum extension of a DPPE lipid chain of 19.1 Å.[43] This indicates that the chains are fully extended, with no interdigitation occurring between the leaflets, and that the lipids are not tilted with respect to the bilayer normal, as in the case of many phosphatidylcholine lipids.[23] The bilayer roughness is comparable to DPPC single bilayers deposited on silicon, whilst the coverage is higher.[6] The transition to the fluid phase was first observed between 65.5 and 74.8 °C, marked by the decrease in the thickness of the chain-region. Overall, the chain-region decreased by 8 Å. This is consistent with the transition from the ordered gel phase to the disordered fluid phase. The thickness continued decreasing up to the highest temperature measured of 79.2 °C. With other DPPE systems the transition has been observed to be an abrupt transition rather than one occurring over a temperature range. The transition in DPPE vesicles in solution occurs at 64 °C.[44] The fact that the transition here occurs over a large temperature range could be due to electrostatic forces from the substrate inhibiting the bilayer freedom.

Table 1 Scattering length densities used in modelling of DPPE bilayer samples. All values are from ref. 6, except for PE head-group (from ref. 53) and cholesterol (from ref. 54)

Material	SLD/10^{-6} Å^{-2}
Si	2.07
SiO_2	3.41
H_2O	−0.56
D_2O	6.35
Palmitoyl chain $C_{30}H_{62}$	−0.41
PE head-group $C_7H_9O_8PN$	2.66
Cholesterol	0.22

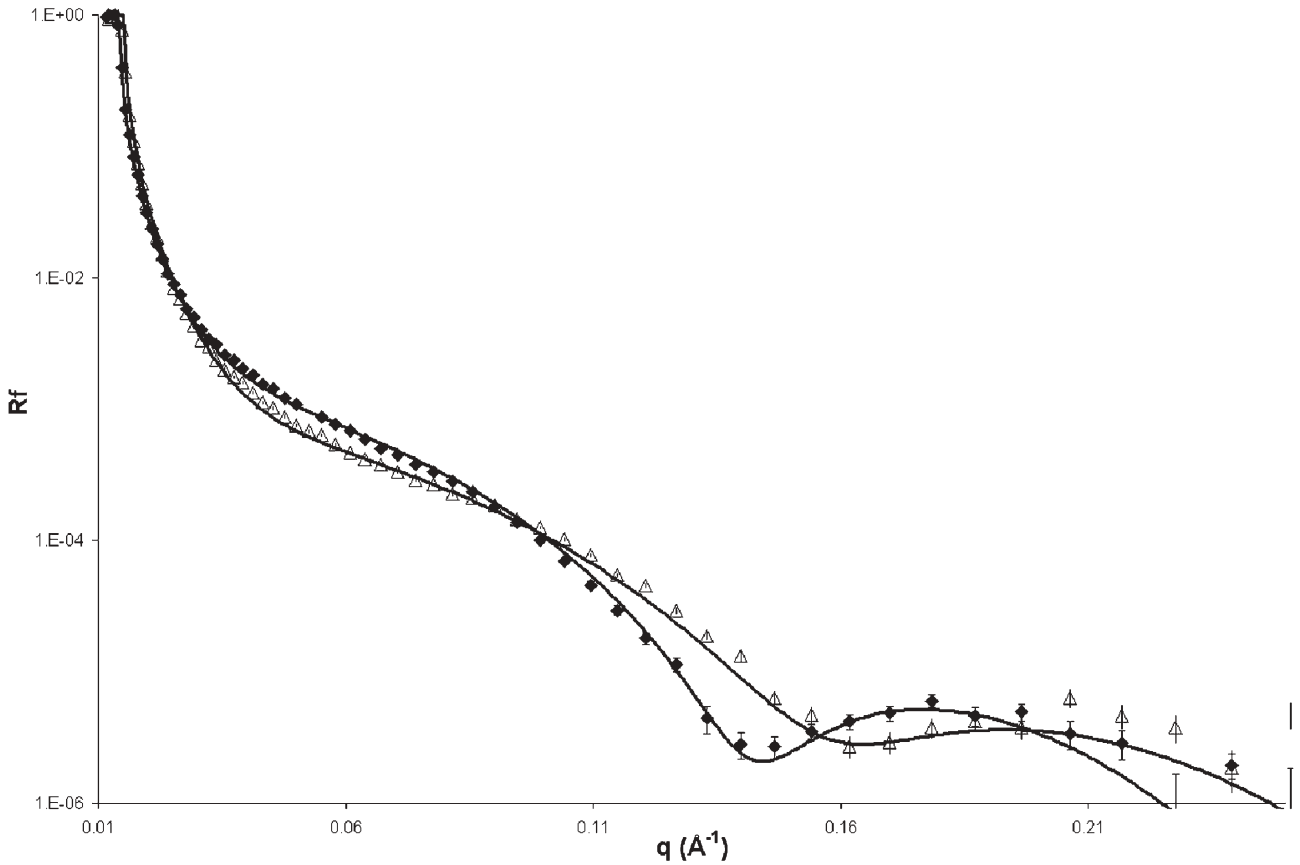

Fig. 1 Reflectivity profiles of a single DPPE bilayer at 25 (♦) and 79 °C (△) and best fit to the data (continuous lines).

Phase-behavior of DPPE double bilayers: gel phase

The structure and stability of the DPPE double planar bilayer was determined at gel phase temperatures between 25.2 °C and 62.9 °C. Fitted reflectivity profiles at three intermediate temperatures are shown in Fig. 2. The gel phase structure is given in Table 3.

The analysis indicates a well defined gel phase double bilayer structure with similar thickness, coverage and roughness parameters for both bilayers. The thickness and roughness of the bilayers were comparable to double those of monolayers measured by other techniques, which had a monolayer thickness of 27 Å,[45] chain-region thickness of 19 Å and a roughness of 4 Å.[43] As in the case of the single bilayer, both bilayers had a chain-region thickness comparable to double the maximum extension of DPPE chains of 19.1 Å.[43] The similarity of the bilayer to twice the monolayer thickness indicated that the lipid chains are not tilted in any way and have little or no interdigitation between the leaflets. It is expected that the leaflets of the bilayer retain the monolayer structure from which they were deposited, with no rearrangement occurring upon deposition.

Table 2 Fitted parameters of DPPE single bilayer. All values are in Å unless otherwise specified. dw is the water layer separating the lower bilayer from the solid substrate, Db is the bilayer thickness, Dc the chain region thickness, Rou is the average bilayer roughness and Cov is the bilayer coverage

Temperature/°C	dw	Db	Dc	Rou	Cov (%)
25.2	6 ± 1	54 ± 2	39 ± 2	7 ± 2	90 ± 2
47.3	6 ± 1	54 ± 2	39 ± 2	7 ± 2	91 ± 2
61.8	6 ± 1	54 ± 2	39 ± 2	7 ± 2	90 ± 2
65.5	6 ± 1	54 ± 2	39 ± 2	7 ± 2	91 ± 2
74.8	5 ± 1	51 ± 2	36 ± 2	8 ± 2	92 ± 2
79.2	5 ± 1	48 ± 2	32 ± 2	8 ± 2	89 ± 2

Phase-behavior of DPPE double bilayers: fluid phase

The sample was measured at fluid phase temperatures between 64.1 °C and 84.0 °C and then upon cooling down to 67 °C. Between 67.4 °C and 69.5 °C, a small Bragg peak was observed in the reflectivity profile at a momentum transfer (q) of 0.12 $Å^{-1}$ (Fig. 3). It occurred just above the gel-to-fluid transition temperature of the vesicles (64 °C).[44] Narrow Bragg diffraction peaks are not normally observed in the reflectivity profiles of double bilayer samples. The appearance of the peak is surprising, especially as the overall shape of the reflectivity profile indicates a high coverage double bilayer profile rather than a single bilayer (*cf.* Fig. 1). The peak shifted to higher q when raising the temperature, indicating that the repeat unit becomes thinner. The peak does not disappear when the sample is cooled back to 25 °C, indicating the formation of an irreversible repeat-unit structure. These results were reproducible, as three experiments were performed on different samples and at different times and all gave the same result.

It is unlikely that an inverted hexagonal structure has been formed, as the d spacing from the position of the Bragg peak

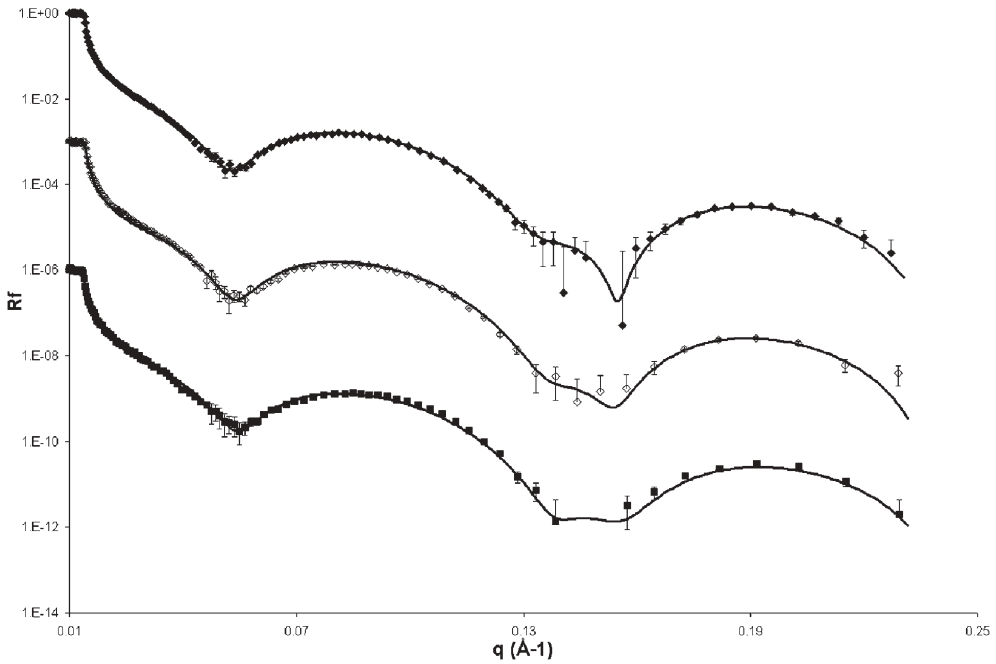

Fig. 2 Fitted reflectivity profiles of DPPE double bilayers at 25.2 °C (◆), 47.3 °C (◇) and 62.5 °C (■). Profiles have been shifted along the *y*-axis for clarity.

Table 3 Gel phase structural parameters of DPPE double bilayer. The prefix u refers to the upper bilayer and l the lower. dw is the water layer thickness separating the lower bilayer from the substrate, Db is the bilayer thickness, Dc is the chain region thickness, Rou is bilayer roughness, Cov is the bilayer coverage and Dw is the water layer thickness separating the two bilayers. All values are in Å unless otherwise specified. The error values are the error determined by modelling

	dw	lDb	lDc	lRou	lCov	Dw	uDb	uDc	uRou	uCov
Gel temperatures	13 ± 1	49 ± 2	36 ± 1	3 ± 1	98 ± 2	16 ± 2	51 ± 2	37 ± 1	5 ± 2	100 ± 1%

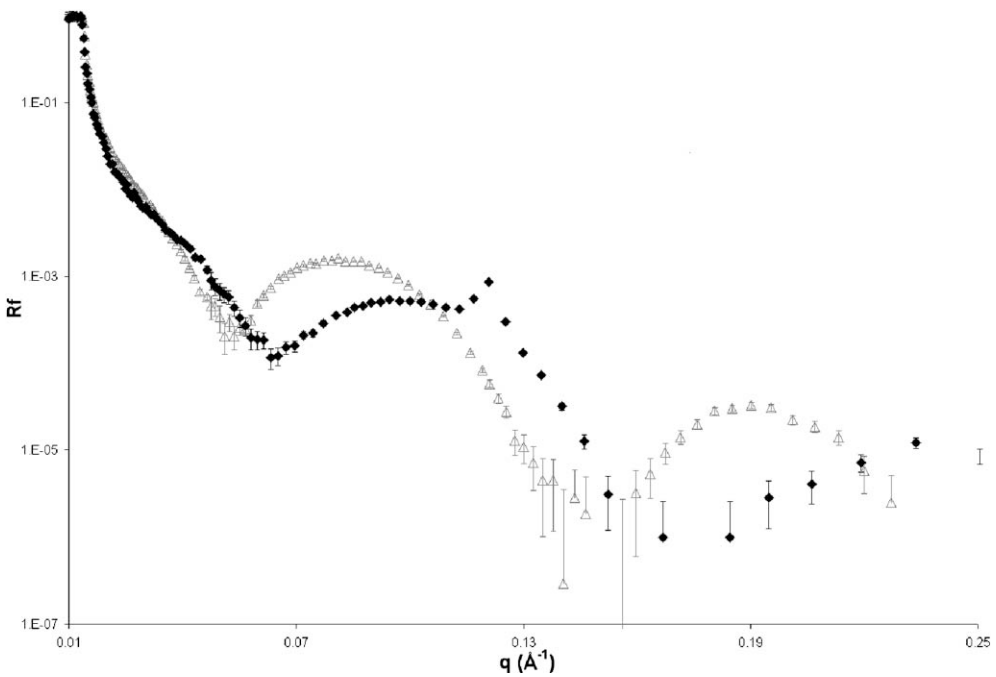

Fig. 3 Reflectivity profiles of DPPE double bilayer at 74.4 °C (◆) and initial 25.2 °C (△). The Bragg peak is clearly visible in the high temperature profile. The shift in the position of the profiles as a function of temperature is visible.

Table 4 Bragg peak position, *d* spacing and thickness of upper (uDb) and lower (lDb) bilayer with temperature. UDb and lDb were obtained by fitting the profile whilst ignoring the Bragg peak. The error in the Bragg peak position is ± 0.01

Temperature/°C	*q* Bragg peak/Å^{-1}	*d* spacing	lDb	uDb
69	0.120	52	47 ± 1	49 ± 1
74	0.121	52	42 ± 1	41 ± 1
80	0.123	51	42 ± 1	42 ± 1
84	0.123	51	41 ± 1	41 ± 1
76	0.122	52	41 ± 1	44 ± 1
74	0.123	51	41 ± 1	43 ± 1
70	0.119	53	41 ± 1	44 ± 1
67	0.119	53	43 ± 1	45 ± 1
64	0.104	60	47 ± 1	49 ± 1
61	0.102	62	50 ± 1	52 ± 1
64	0.104	60	50 ± 1	51 ± 1
29	0.100	63	50 ± 1	53 ± 1

(52 ± 1 Å for the fluid phase and 62 ± 1 Å for the gel phase) is closer to that of a planar bilayer structure rather than an inverted hexagonal structure. In fact, inverted hexagonal structures tend to have large repeat-spacing due to the large diameter of the initial water channel, which has been found to be 25 Å for DDPE (di-C_{12}), 44 Å for DAPE (di-C_{20})[24] and 30 Å for POPE[46] in aqueous dispersions. The fluid-to-inverted hexagonal transition of DPPE (123 °C[24]) is also known to occur at a much higher temperature than the rearrangement temperature here.

The presence of the Bragg peak in the reflectivity profiles greatly complicated the analysis. While it was clearly not possible to fit the data with a double bilayer model, no satisfactory fit was obtained even when using a pure multilamellar system. To fit the peak and the overall profile, it was necessary to have a high-coverage double bilayer and a lamellar stack composed of 11 bilayers of low coverage (11%) above it. Table 4 gives a summary of the parameters used to fit the data at different temperatures, neglecting the presence of the Bragg peak. The position of the Bragg peak at each temperature is also given. The best fit to the data taking into account the Bragg peak is shown in Fig. 4. What is surprising is that it is necessary to include a double bilayer with a full coverage in the lamellar stack model. In the fit shown the instrumental resolution has been taken into account.

The most plausible interpretation is that as the area per molecule of the lipid increases with the transition to the fluid phase, the high bilayer coverage forces the bilayer to rupture, forming a low coverage repeat-stacking unit over certain areas of the surface, while others remain covered with a high-coverage double bilayer. If the islands are bigger than the coherence length of the beam (about 10 μm in the used configuration) the reflectivity has to be weighted according to the equation: $|r|^2 = \Phi_B |r|_B^2 + \Phi_M |r|_M^2$, where the subscripts B and M refer to the double bilayer and multilamellar islands, respectively, and Φ_B and Φ_M are the volume fractions. Estimation of Φ_B and Φ_M is not straightforward and was not attempted as it is outside the scope of this work.

What we can infer from the data is that: the Bragg peak occurs above T_m; permanent structural change occurs; the

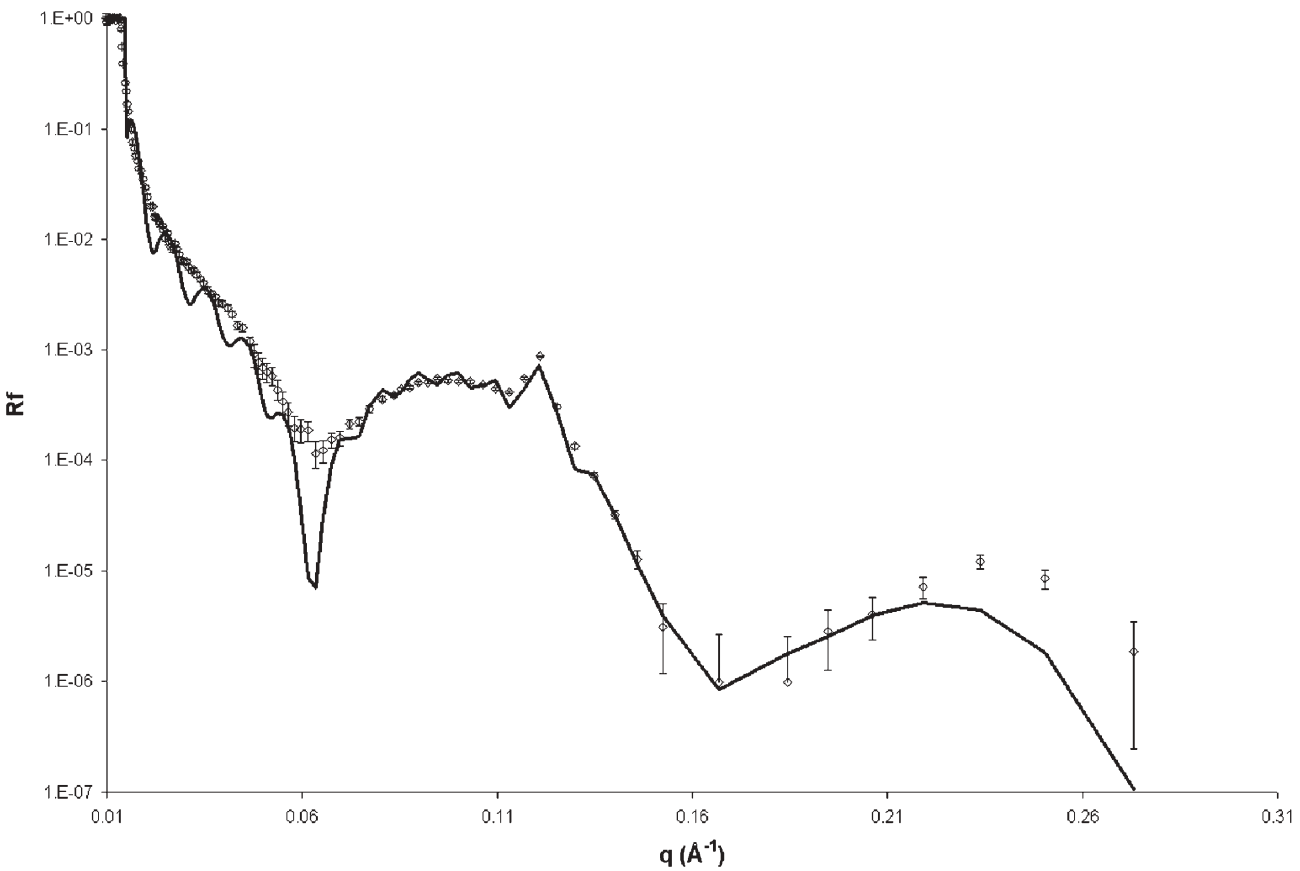

Fig. 4 Best fit of reflectivity profile of DPPE double bilayer in the fluid phase (74.4 °C) after appearance of Bragg peak. See text for details.

Bragg peak q position shifts with temperature. Fitting by neglecting the presence of the Bragg peak indicates a transition into the fluid phase.

A comparison may be attempted between the parameters used to model the data in the gel phase (absence of the Bragg peak) and fluid phase (presence of the Bragg peak). The coverage parameters for the double bilayer are identical; roughness is identical; it is necessary to use fluid phase chain thickness for the double bilayer and repeat bilayer to achieve a good fit (this shows that there has been a transition to the fluid phase as suspected). Finally the thicknesses of both water layers (dw, Dw) have decreased slightly. The water layer in the repeat units is thinner than Dw thickness by 3 Å.

The observation of a reduction in chain thickness without a change in the bilayer roughness agrees with the behaviour observed in the single bilayer sample.

Phase-behavior of 9 : 1 DPPE/cholesterol double bilayer

The reflectivity of a 9 : 1 DPPE/cholesterol double bilayer sample was measured between 25 °C and 62 °C, upon cooling back to 25 °C and then upon reheating to 53 °C. Selected fitted reflectivity profiles are given in Fig. 5 and parameters used to fit the data are listed in Table 5.

Between 25.3 °C and 47.1 °C the structure was consistent with two gel phase bilayers. The structural parameters were comparable to those of the double and single bilayer samples mentioned in this article. Upon heating from 52.2 °C to 56.4 °C the reflectivity profile underwent a large change. The characteristically curved fringes (that indicate the presence of a double bilayer structure) became flat, with the overall profile adopting that usually associated with a single bilayer structure.[5] The profile shape was retained even when cooled back to the initial 25 °C. When the data was analysed, the change from a double bilayer to a single bilayer was indeed found to have occurred. Between 52.2 °C and 56.4 °C, almost all of the upper bilayer detached. By 61.6 °C the sample consisted only of a single bilayer. The detachment of the upper bilayer occurred 7 °C below the gel-to-fluid transition temperature of DPPE vesicles. The lower bilayer structure remained relatively constant throughout the detachment.

Although the presence of 10 mol% cholesterol does not significantly alter the gel phase structure, it completely destabilises the floating bilayer near the gel-to-fluid phase transition temperature. It is possible that cholesterol lowers the temperature at which the gel-to-fluid transition occurs in the upper bilayer. If the bilayer becomes fluid at 56 °C, then this would allow the lipids to have sufficient mobility and detach. The interaction of cholesterol with lipids varies appreciably with the structure of the head-group and the structure and length of the hydrocarbon chains.[31] The lowering of the transition temperature by cholesterol has previously been

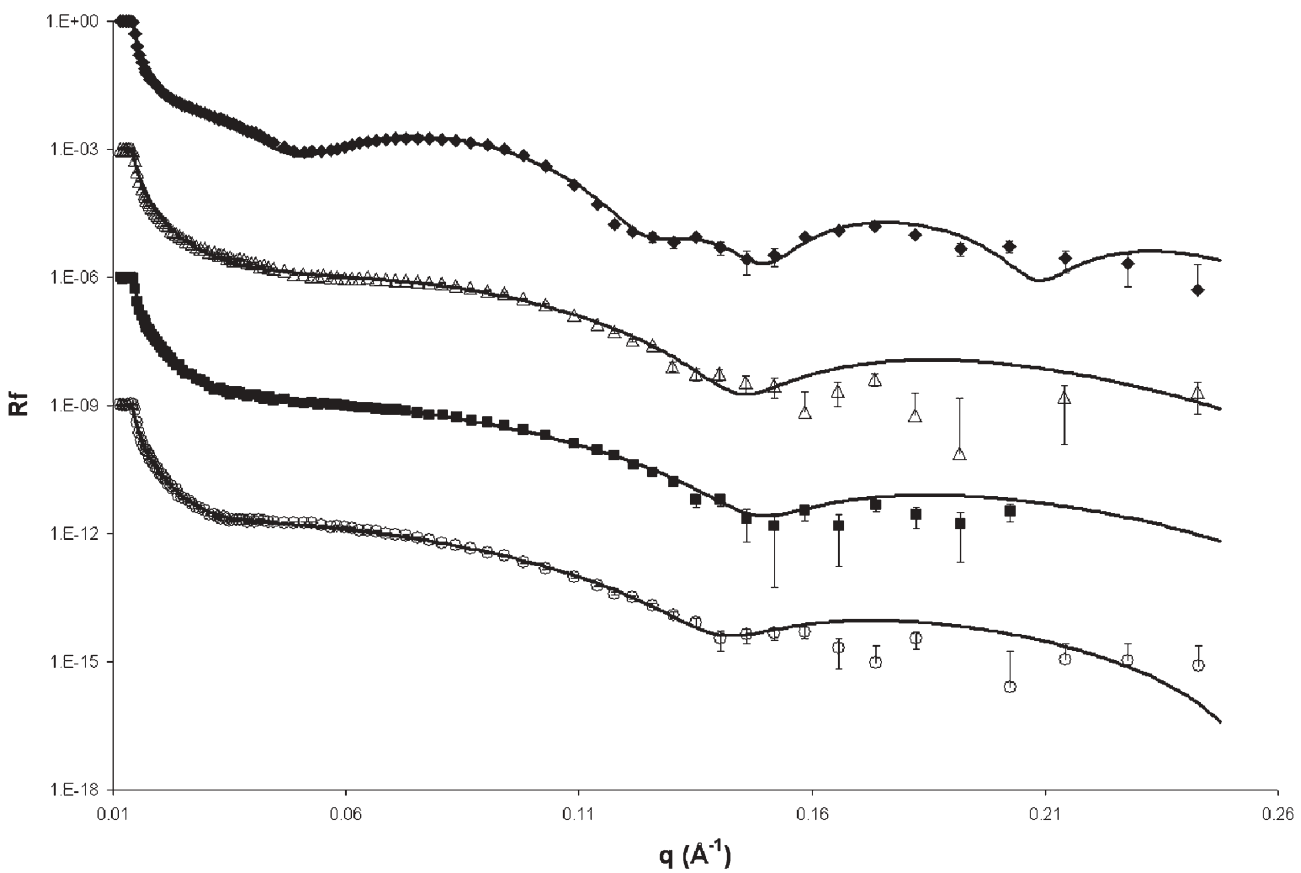

Fig. 5 Fitted reflectivity profiles of 9 : 1 DPPE/cholesterol double bilayer at 25.3 °C (◆), 56.1 °C (△), 61.6 °C (■) and 25.2 °C (upon cooling) (○). Profiles have been shifted down the y-axis for clarity.

Table 5 Fitted parameters of reflectivity of DPPE double bilayers with 10 mol% cholesterol. All values are in Å unless otherwise specified.

	Temperature/°C	dw	lDb	lDc	lRou	lCov	Dw	uDb	uDc	uRou	uCov
Heating	25	12 ± 1	51 ± 2	37 ± 1	5 ± 2	87 ± 2	23 ± 1	47 ± 2	37 ± 1	5 ± 2	100 ± 2
	34	11 ± 1	51 ± 2	37 ± 1	3 ± 2	89 ± 2	22 ± 1	52 ± 2	37 ± 1	5 ± 2	100 ± 2
	43	11 ± 1	50 ± 2	36 ± 1	3 ± 2	90 ± 2	21 ± 1	51 ± 2	37 ± 1	5 ± 2	100 ± 2
	47	11 ± 1	50 ± 2	36 ± 1	5 ± 2	89 ± 2	22 ± 1	49 ± 2	37 ± 1	6 ± 2	100 ± 2
	52	9 ± 1	49 ± 2	35 ± 1	7 ± 2	88 ± 2	22 ± 1	51 ± 2	36 ± 1	7 ± 2	100 ± 2
	56	11 ± 2	52 ± 2	38 ± 1	3 ± 2	95 ± 2	18 ± 9	50 ± 9	35 ± 7	6 ± 12	7 ± 5
	61	12 ± 1	51 ± 2	37 ± 1	4 ± 2	90 ± 2					
Cooling	56	12 ± 1	53 ± 2	37 ± 1	5 ± 2	91 ± 2					
	52	13 ± 1	52 ± 2	37 ± 1	4 ± 2	93 ± 2					
	47	13 ± 1	53 ± 2	38 ± 1	3 ± 2	91 ± 2					
	43	14 ± 1	54 ± 2	39 ± 1	4 ± 2	91 ± 2					
	34	14 ± 1	53 ± 2	38 ± 1	5 ± 2	91 ± 2					
	25	14 ± 1	53 ± 2	38 ± 1	5 ± 2	92 ± 2					
Heating	34	15 ± 1	51 ± 2	37 ± 1	7 ± 2	92 ± 2					
	43	15 ± 1	51 ± 2	37 ± 1	7 ± 2	92 ± 2					
	47	15 ± 1	51 ± 2	37 ± 1	7 ± 2	92 ± 2					
	52	15 ± 1	51 ± 2	37 ± 1	7 ± 2	91 ± 2					

observed with vesicles of other types of phosphatidylethanolamines, where cholesterol progressively reduced the transition temperature up to concentrations of 20 mol%.[33,31] 10 mol% of cholesterol has also been observed to lower the transition temperature of the long-chained DSPE lipid by 4 °C.

One of the main considerations for the cause of the detachment is the molecular shape of the DPPE lipid. The bulk shape that lipids adopt under a given set of conditions can be rationalised by considering the geometric packing of the lipids, which in turn can be described by the shape-factor characteristic of the individual lipid molecule under these conditions.[46] The DPPE molecule is conically shaped due to the small amine head-group and large chain-area per molecule. This would be expected to favour a spherical shape over a planar shape. If the cholesterol is located predominantly in the chain region of the bilayer, as in the case of phosphatidylcholines,[42] then this could be expected to increase the chain-to-tail size ratio by packing its hydrophobic bulk close to the DPPE tail region. This would increase the instability of the planar structure. For this to be the case then the miscibility of the DPPE and cholesterol molecules needs to be considered. It has been empirically found that miscibility of cholesterol with any lipid is inversely related to the characteristic degree of order or tightness of packing of the phospholipids at a given temperature and phase state. Phospholipids with strong intermolecular interactions tend to exclude cholesterol from the bilayer above certain concentrations. Phosphatidylethanolamine head-groups have strong attractive electrostatic and hydrogen bonding.[31,33] In vesicles of phosphatidylethanolamines and cholesterol, the strong lipid inter-head-group electrostatic and hydrogen bonding interactions favour lipid–lipid interactions over lipid–cholesterol interactions.[47] Formation of domains of cholesterol has been observed only at concentrations of 35 mol% or above.[48] This suggests that in the sample containing 10 mol% cholesterol none or very limited domain formation of cholesterol is likely to be present. The DPPE and cholesterol would then be expected to have significant miscibility, which would increase the conical shape of the DPPE, destabilising the planar bilayer structure. Cholesterol in the fluid phase exhibits increased miscibility than when in the gel phase.[33,31] If the cholesterol was reducing the gel-to-fluid transition temperature, then the increased miscibility of cholesterol and DPPE in the fluid phase could be an explanation of the detachment of the upper bilayer.

Another factor that needs to be considered is that the detachment is caused by cholesterol increasing the fluctuations present in the bilayer. It has been predicted that the detachment of a bilayer from a substrate, or another membrane, is driven predominantly by thermally excited fluctuations in the bilayer.[49,50] The fluctuations overcome the attractive Van der Waals and electrostatic forces[51] that hold the bilayer to the interface. With the double bilayer sample it is unclear at what temperature the fluctuations would overcome the attractive forces. Double bilayers of the phosphatidylcholine DPPC have been heated to temperatures 40 °C above their gel-to-fluid transition temperature without detachment occurring.[17] Even when 10 mol% cholesterol was incorporated, the double bilayer remained stable at fluid phase temperatures.[21] In phosphatidylcholine systems, the inclusion of 8–14 mol% of cholesterol in DMPC has been found to sustain some types of fluctuations of the transition region upon cooling to temperatures of 10 °C lower than T_m.[52] However, the effect of cholesterol on the fluctuations of phosphatidylethanolamine bilayers is unclear in the literature. In the case of the double bilayer sample here, the structural parameters show no indication of increased fluctuations near the detachment temperature. Increased fluctuations would be expected to increase the bilayer roughness parameter and also give rise to increased off-specular scattering. As neither of these cases was observed it is unlikely that increased fluctuations due to the presence of cholesterol are the cause of the detachment. It is more likely that the main factor in the detachment is due to structural driving forces rather than being fluctuation driven.

Acknowledgements

The authors wish to thank R. Cubitt and S. Wood for their help during the measurements, the ESRF optics lab for polishing the silicon blocks and the ILL for providing beam-time.

References

1 L. K. Nielsen, J. Risbo, T. H. Callisen and T. Bjørnholm, *Biochim. Biophys. Acta*, 1999, **1420**, 266.
2 A. L. Plant, *Langmuir*, 1999, **15**, 5128.
3 S. Terrettaz, M. Mayer and H. Vogel, *Langmuir*, 2003, **19**, 5567.
4 M. A. Cooper, A. C. Try, J. Carroll, D. J. Ellar and D. H. William, *Biochim. Biophys. Acta*, 1989, **1373**, 101.
5 T. Charitat, E. Bellet-Amalric, G. Fragneto and F. Graner, *Eur. Phys. J. B*, 1999, **8**, 583.
6 G. Fragneto, F. Graner, T. Charitat, P. Dubos and E. Bellet-Amalric, *Langmuir*, 2000, **16**, 4581.
7 M. Benes, D. Billy, W. T. Hermens and M. Hof, *Biol. Chem.*, 2002, **383**, 337.
8 L. K. Tamm and H. M. McConnell, *Biophys. J.*, 1985, **47**, 105.
9 G. Puu and I. Gustafson, *Biochim. Biophys. Acta*, 1997, **1327**, 149.
10 J. Yang and J. Appleyard, *J. Phys. Chem. B*, 2002, **104**, 8097.
11 M. J. M. Darkes and J. P. Bradshaw, *Acta Crystallogr., Sect. D: Biol. Crystallogr.*, 1999, **D56**, 48.
12 T. Salditt, C. Li and U. Mennicke, *Eur. Phys. J. E*, 2002, **7**, 105.
13 J. Majewski, J. Y. Wong, C. K. Park, M. Seitz, J. N. Israelachvili and G. S. Smith, *Biophys. J.*, 1998, **75**, 2363.
14 M. L. Wagner and L. K. Tamm, *Biophys. J.*, 2000, **79**, 1400.
15 J. Saccani, S. Castano, B. Desbat and D. Blaudezy, *Biophys. J.*, 2003, **85**, 3781.
16 S. Krueger, C. W. Meuse, C. F. Majkrzak, J. A. Dura, N. F. Berk, M. Tarek and A. L. Plant, *Langmuir*, 2001, **17**, 511.
17 G. Fragneto, T. Charitat, E. Bellet-Amalric, R. Cubitt and F. Graner, *Langmuir*, 2003, **19**, 7695.
18 A. V. Hughes, S. J. Roser, M. Gerstenberg, A. Goldar, B. Stidder, R. Feidenhans'l and J. Bradshaw, *Langmuir*, 2002, **18**, 8161.
19 J. Daillant, E. Bellet-Amalric, A. Braslau, T. Charitat, G. Fragneto, F. Graner, S. Mora, F. Rieutord and B. Stidder, *Proc. Natl. Acad. Sci. U. S. A.*, 2005, **102**, 11639.
20 B. Stidder, G. Fragneto and S. J. Roser, *Langmuir*, 2005, **21**, 9187.
21 B. Stidder, G. Fragneto, R. Cubitt, A. V. Hughes and S. J. Roser, *Langmuir*, 2005, **21**, 8703.
22 A. Blume, *Biochemistry*, 1980, **19**, 4908.
23 T. J. McIntosh, *Biophys. J.*, 1980, **29**, 237.
24 J. M. Seddon, G. Cevc and D. Marsh, *Biochemistry*, 1983, **22**, 1280.
25 P. E. Harper, D. A. Mannock, R. N. A. H. Lewis, R. N. McElhaney and S. M. Gruner, *Biophys. J.*, 2000, **81**, 2693.
26 J. M. Seddon and R. H. Templer, *New Sci.*, 1991, **1769**, 45.
27 I. W Hamley, *Introduction to soft matter*, John Wiley and Sons Ltd, Bognor Regis, England, 2000.
28 D. C. Turner and S. M. Gruner, *Biochemistry*, 1992, **31**, 1340.
29 K. Harlos and H. Eibl, *Biochemistry*, 1980, **20**, 2888.
30 P. L. Yeagle, *Biochim. Biophys. Acta*, 1985, **822**, 267.
31 T. P. W. McMullen, R. N. A. H. Lewis and R. N. McElhaney, *Biochim. Biophys. Acta*, 1999, **1416**, 119.
32 R. Marinov and E. J. Dufourc, *J. Chim. Phys. Phys.-Chim. Biol.*, 1995, **92**, 1727.
33 T. P. W. McMullen and R. N. McElhaney, *Biochemistry*, 1997, **36**, 4979.
34 S. Alexandre, G. Cole, S. Coutard, C. Monnier, V. Norris, W. Margolin, X. Yu and J. M. Valleton, *Colloids Surf., B*, 2002, **23**, 391.
35 D. Gidalevitz, Y. Ishitsuka, A. S. Muresan, O. Konovalov, A. J. Waringi, R. I. Lehreri and K. Y. C. Lee, *Proc. Natl. Acad. Sci. U. S. A.*, 2003, **100**, 6302.
36 C. E. H. Berger, K. O. Van der Werf, R. P. H. Kooyman, B. G. de Grooth and J. Greve, *Langmuir*, 1995, **11**, 4188.
37 J. R. Vig, *J. Vac. Sci. Technol., A*, 1985, **3**, 1027.
38 J. Penfold, R. M. Richardson, A. Zarbakhsh, J. R. P. Webster, D. G. Bucknall, A. R. Rennie, R. A. L. Jones, T. Cosgrove, R. K. Thomas, J. S. Higgins, P. D. I. Fletcher, E. Dickinson, S. J. Roser, I. A. McLure, A. R. Hillman, R. W. Richards, E. J. Staples, A. N. Burgess, E. A. Simistero and J. W. White, *J. Chem. Soc., Faraday Trans.*, 1997, **93**, 3899.
39 J. Penfold and R. K. Thomas, *J. Phys.: Condens. Matter*, 1990, **2**, 1369.
40 M. Born and E. Wolfe, *Principles of Optics*, Pergamon Press, Oxford, UK, 1989.
41 R. Cubitt and G. Fragneto, *Appl. Phys. A: Mater. Sci. Process.*, 2002, **74**, S329.
42 A. Leonard, C. Escrive, M. Laguerre, E. Pebay-Peyroula, W. Néri, T. Pott, J. Katsaras and E. J. Dufourc, *Langmuir*, 2001, **17**, 2019.
43 M. Thoma, M. Schwendler, H. Baltes, C. A. Helm, T. Pfohl, T. Riegler and H. Mohwald, *Langmuir*, 1996, **12**, 1722.
44 Y. Racansky, D. Valachovic and P. Balgavy, *Acta Phys. Slovaca*, 1987, **37**, 166.
45 J. M. Solletti, M. Botreau, F. Sommer, W. L. Brunat, S. Kasas, T. M. Duc and M. R. Celio, *Langmuir*, 1996, **12**, 5379.
46 M. Rappolt, A. Hickel, F. Bringezu and K. Lohnery, *Biophys. J.*, 2003, **84**, 3111.
47 H. Ohvo-Rekila, B. Ramstedt, P. Leppimaki and J. P. Slotte, *Prog. Lipid Res.*, 2002, **41**, 66.
48 J. J. Cheetham, E. Wachtel, D. Bach and R. M. Epand, *Biochemistry*, 1989, **28**, 8928.
49 R. Lipowsky and S. Leibler, *Phys. Rev. Lett.*, 1989, **56**, 2541.
50 U. Seifert and R. Lipowsky, *Dynamical phenomenon at surfaces, interfaces and membranes*, Nova Science, New York, USA, 1993.
51 W. Z. Helfrich, *Z. Naturforsch., A: Phys. Phys. Chem. Kosmophys.*, 1977, **33**, 305.
52 K. Mortensen, W. Pfeiffer, E. Sackmann and W. Knoll, *Biochim. Biophys. Acta*, 1988, **945**, 221.
53 T. L. Kuhl, J. Majewski, J. Y. Wong, S. Steinberg, D. E. Leckband, J. N. Israelachvili and G. S. Smith, *Biophys. J.*, 1998, **75**, 2352.
54 B. Deme, *J. Phys. Chem. B*, 1997, **101**, 8250.

